AIAA JOURNAL
Vol. 43, No. 3, March 2005

Narrow-Linewidth Ultraviolet Source for Rayleigh and Raman Applications

Lipeng Qian,* Sohail H. Zaidi,† and Richard Miles‡
Princeton University, Princeton, New Jersey 08544

A pulsed, high-efficiency, narrow-linewidth ultraviolet source is developed to explore its potential for Rayleigh and Raman applications. A mercury lamp is driven with a high-voltage (30-kV), 2-ns-long, high-repetition-rate pulse supply that produces a high average power train of light pulses. Each pulse in the train has a time-varying spectrum that narrows to a single spectral line after 100 ns or so. This ultranarrow line output falls at 254 nm and lends itself to filtered Rayleigh and filtered Raman scattering measurements in conjunction with a mercury vapor filter. The performance of the mercury lamp has been characterized by operating the lamp in different configurations and at various operating conditions. It was found that the lamp with the external electrodes performs better than that with inner electrodes. The possibility of obtaining other Hg-UV lines, particularly 185-nm radiation, has also been explored. The suitability of this lamp for Raman measurements has been tested by recording vibrational Raman spectrum for methanol. Filtered Rayleigh signals were also obtained for CO_2 at various gas pressures.

I. Introduction

AVAILABILITY of intense, tunable, single-frequency, narrow-linewidth lasers along with the atomic notch filters have greatly improved the techniques used for classical Rayleigh and Raman measurements. Filtered Rayleigh scattering is an extension of the Rayleigh technique, which has long been used as a tool for flowfield diagnostics. Rayleigh scattering is the strongest nonresonant scattering process but is often interfered with and limited by the elastically scattered light from particles, windows, lenses, and walls. This limitation can be removed by the addition of an atomic or molecular filter in front of the detector. This approach is known as filtered Rayleigh scattering (FRS) and has been extensively used for many practical applications including flow visualization and quantitative measurement of fluid properties in supersonic flows, weakly ionized plasmas, and combusting environments. Recent work shows that the FRS technique can be successfully used with a tunable laser source to capture quantitative planar measurements of gas temperature, pressure, density, and velocity.[1] If the source frequency falls at the center of the atomic or molecular filter spectral blocking region and the gas pressure is known, the filter simultaneously can block background scattering and can record the local temperature in weakly ionized plasmas[2] and combusting gasses.[3] Compared with FRS in the visible and infrared regions, FRS in the ultraviolet is preferred because the Rayleigh scattering cross section is proportional to the fourth power of the frequency. The mercury vapor transition at 254 nm is particularly useful for this application because mercury has a high vapor pressure and high atomic mass, and so an optically thick atomic vapor cell has sharp edges and so it acts very much like a notch filter.[4]

One of the restrictions in performing ultraviolet FRS is the availability of light source in that region. To use the mercury vapor filter at 254 nm, the illumination source needs to be narrow linewidth and at the same frequency. Frequency-tripled Ti:sapphire and alexandrite lasers have been successfully employed for this purpose, but these laser systems require injection-locking, active frequency control, and they produce relatively low light levels in this regime. Because of these practical problems, the possibility of using a mercury vapor lamp as a replacement for these laser sources becomes very attractive, but for it to be useful as a source for FRS, the linewidth of the mercury lamp must be as narrow as or narrower than the mercury absorption filter.

One of the main limitations of Rayleigh scattering is that the signal does not contain species-specific information. Spontaneous Raman scattering can provide information on species concentration.[5] Pure rotational Raman scattering has about one order of magnitude larger cross section than the vibrational counterpart. However, the pure rotational spectrum resides in close proximity to the laser line due to the small energy spacing between the rotational states, so that spectral rejection of the elastic background is a severe challenge. Atomic filter techniques can be used to overcome this problem.[6–9] Tunable Ti:sapphire lasers in the infrared region with the Rb filter and frequency-tripled Ti:sapphire in the ultraviolet with the Hg filter have been employed to demonstrate this capability. Again the laser systems require injection locking, are complicated and expensive, and are difficult to operate. Like Rayleigh scattering, the Raman scattering cross section scales as the fourth power of the scattering frequency; thus, it is preferable to operate in the ultraviolet region. Because the Raman signals are weak compared to their Rayleigh counterpart, high-average-power sources and detectors with high quantum efficiency are even more critical. In the ultraviolet region, charge-coupled device cameras can have quantum efficiencies as high as 60% (Ref. 10). If a high average power, very narrow linewidth, inexpensive ultraviolet light source that is centered on an atomic absorption line can be developed, it could have a significant impact on both Rayleigh and Raman detection techniques.

Low-pressure arc discharges in mercury–inert gas mixtures have been studied for years. They are efficient sources for conversion of electrical energy into radiation through excitation of the resonant lines of the mercury atom at 185 and 254 nm (Ref. 11). Commercial mercury lamps usually operate with dc or low-frequency ac glow discharge. Studies have shown that the use of a short-pulse discharge in these mercury inert gas mixtures can enhance the output efficiency of the ultraviolet radiation.[12–14] For instance, a 12.0–82.0-ns pulse discharge in the form of a high-speed ionization wave in a mixture of mercury vapor and argon has been studied by Vasilyak et al.[15] With the use of a pulser rather than a continuous discharge, it was possible to increase the excited population of the resonant state of the mercury atom by more than a factor of 10. The research reported here also uses short, pulsed excitation, but in the 2.0-ns regime. This pulse is significantly shorter than the emission lifetime of the

Presented as Paper 2004-20 at the AIAA 42nd Aerospace Sciences Meeting, Reno, NV, 5–8 January 2004; received 19 March 2004; revision received 26 October 2004; accepted for publication 26 October 2004.

*Graduate Student, Department of Mechanical and Aerospace Engineering. Student Member AIAA.
†Research Staff Member, Department of Mechanical and Aerospace Engineering. Member AIAA.
‡Professor, Department of Mechanical and Aerospace Engineering. Fellow AIAA.

excited state, so that the time evolution of the emitted resonance radiation can be followed. It has been observed that the short-time radiation has multiple lines associates with many mercury vapor transitions, but after 100.0 ns or so, only the lines at 254 and 185 nm persisted because they were optically trapped in the vapor. This time-delayed radiation is exceptionally narrow linewidth, reflecting the cold mercury atom temperature; thus, through time gating, the mercury lamp can be made to function as an ultranarrow source.

II. Experimental Setup

The mercury lamp used in this study was a cylindrical quartz tube with electrodes on each end of it. The lamp has a cold tip that was filled with a very small quantity of liquid mercury. The tip temperature was controlled and maintained as the lowest temperature point of the discharge tube. The temperature of the cold tip controlled the mercury vapor pressure. A schematic diagram of the tube is shown in Fig. 1. The discharge tube also had an outlet valve, which was used to change the inert gas fill and was closed during the experiment. The inner diameter of the tube was 1.0 cm, and the interelectrode gap was about 6.0 cm. The discharge tube was surrounded by a grounded copper screening foil. The screening foil was used to reduce the impedance of the discharge circuit, to lower the electronic noise arising from the discharge, and to facilitate breakdown in the tube. The copper screening had an opening of about 1 cm^2, which was used for the emission of the optical radiation from the lamp.

The discharge tube was excited by a high-voltage, high-frequency electrical pulser capable of generating 2.0-ns, 30.0-kV pulses, each having a rise time of about 1.0 ns. These high-voltage pulses were generated across a 400-Ω load at a repetition rate of up to 100.0 kHz. The device used a proprietary switching diode in an inductor–resistor–capacitor (L–R–C) circuit to generate 10.0-kV pulses. In the current experiment, measurements were made at a pulse repetition rate of 11.0 kHz. The lamp was also operated in the pulse burst mode, where the repetition rate of the pulse package was kept at 1.0 kHz, and 10 pulses were generated at a 100.0-kHz rate in each package.

To measure the spectrum of the mercury lamp, the light collected from the optical opening of the lamp was focused onto a Model SP-500 I Acton Research spectrometer. This spectrometer had a 2.0-m path length and a 2400-g/mm grating that was coated for UV detection. The minimum slit width of the spectrometer was 10.0 μm, and with this width, a maximum resolution of 0.05 nm was achieved. The spectrometer was used in conjunction with a Hamamatsu Model R1477 photomultiplier, which had ~25% quantum efficiency at 254 nm. The line shapes of the radiation decay were observed on an oscilloscope, and the spectra were recorded through a gated integrator.

III. Experimental Results

In these experiments, a homogeneous discharge was observed. As mentioned in Refs. 12–15, the shorter excitation time provided higher efficiency for the 254-nm radiation. Also, because the pulse excitation time was significantly shorter than the lifetime of the excited states,[16] it was possible to observe the time decay of the different radiation lines. The emission spectrum of the pulsed mercury discharge lamp with 3.0 torr of helium and 80.0 mtorr of mercury is shown in Fig. 2. The spectrum was integrated for 3.0 μs. This broad spectrum is characteristic of the dc glow discharge Hg lamp, and

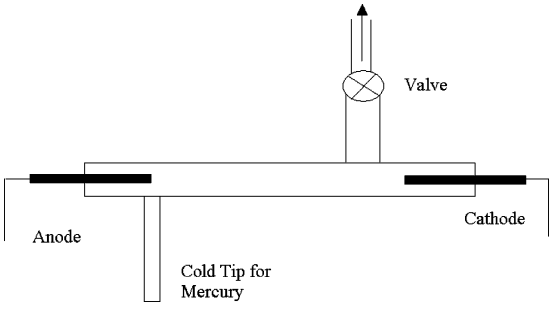

Fig. 1 Mercury lamp design.

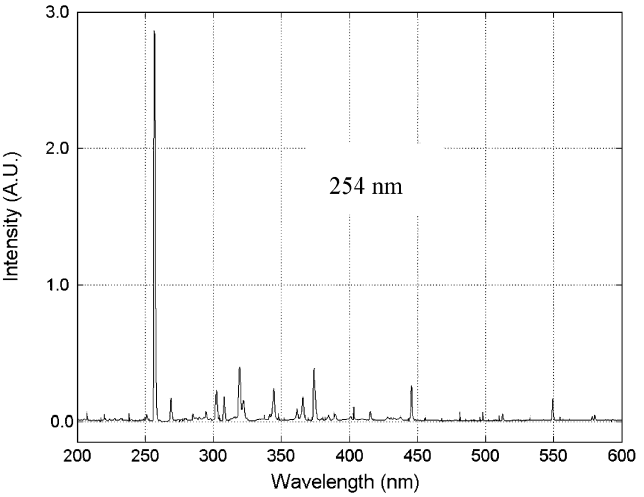

Fig. 2 Spectrum of the Hg lamp with 3-μs integration time (3.0-torr He, 80.0-mtorr Hg).

the multiple spectral lines seen here make such a lamp poor source for FRS, even though more than 60% of the shot energy lies in the 254-nm line.

Figure 3 shows the time evolutions at 254, 313, and 365 nm, which correspond to the transitions of 6^3P_1–6^1S_0, 6^3D_2–6^3P_1, and 6^3D_3–6^3P_2 transition. Note that 6^1S_0 is the ground state of mercury. These lines were selected because they were the strongest observed in the spectrum. The time constant of the 254-nm line decay was estimated by fitting a curve and was found about 7.0 μs. Decay times of all of the other lines were below 200 ns. This difference was explained primarily by optical trapping. Because the emitted photons were reabsorbed by the Hg atoms and were reemitted again and again, the decay time of the radiation at 254 nm was much longer than the lifetime of that excited state. Because the decay time of the 254 line was much longer than those of the other lines, it was possible to obtain pure 254-nm radiation by delaying the integration time by a few hundred nanoseconds. Figure 4 shows the spectrum taken following a 200.0-ns time delay.

The spectral distribution is also a function of the inert gas pressure. As a comparison, Fig. 2 shows the spectrum with 3.0 torr of helium and Fig. 5 shows the spectrum with 10.0 torr of helium. Note that the relative intensity of the 254-nm line depends strongly on the gas fill. Approximately 60% increase was observed in the intensity of 254 line as the helium pressure was increased from 3.0 to 10.0 torr.

From experiments, it was observed that the radiation intensity at 254 nm was stronger with helium than with argon, as is shown in Figs. 5 and 6, in which spectra from the Hg lamp were obtained under identical operating conditions for both gases. Note that electron temperature in the discharge was controlled by the ambipolar diffusion. The ambipolar diffusion coefficient for helium was almost 100 times higher than that for argon. In addition, the intensity maximum was related to the mercury vapor pressure in the discharge tube. Figure 7 shows the relative 254-nm radiation intensity under various pressures of argon and helium for a case when the temperature of the cold tip was kept constant at 80.0°C. Because the initial electron temperature of the discharge is dictated by the electrical field/pressure (E/P) value, the intensity of 254-nm radiation also changes with the changing of the filling gas pressure. Figure 7 clearly shows that, for identical operating conditions, the intensity at 254-nm line is two–three times stronger with helium than with argon as the filling pressure varies from 5.0 to 50.0 torr.

The performance of the lamp was also found to depend on the repetition rate of the pulses. Figure 8 shows the 254-nm radiation of a lamp with a 10-torr helium fill at different repetition rates. Normally, the 254-nm radiation intensity decreases with the increase of the repetition rates. Increasing repetition rate increases the gas temperature, which, for a constant pressure, reduces the density of atoms that radiate.

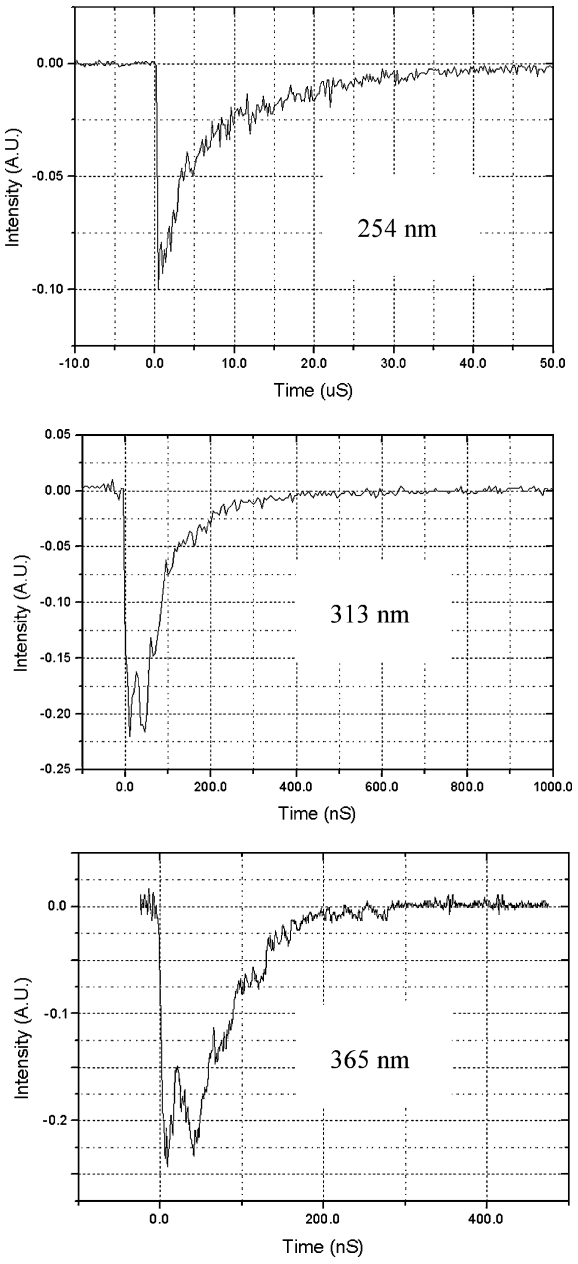

Fig. 3 Pulse shapes at 254, 313, and 365 nm (3.0-torr He, 80.0-mtorr Hg, 3.0-μs integration).

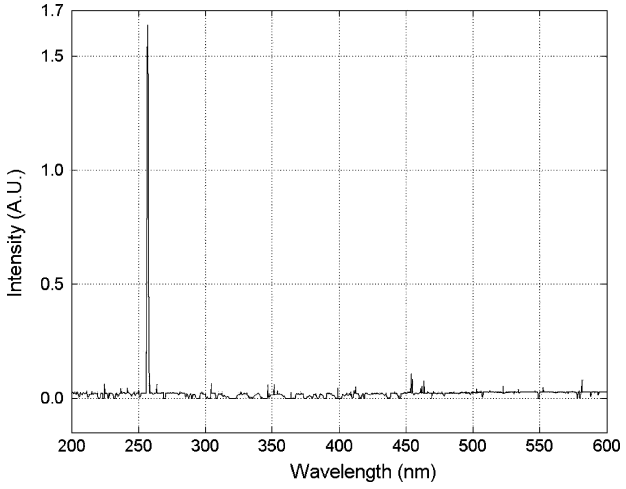

Fig. 4 Spectrum of Hg lamp with 200.0-ns delay (3.0-torr He, 80.0-mTorr Hg, 3.0-μs integration).

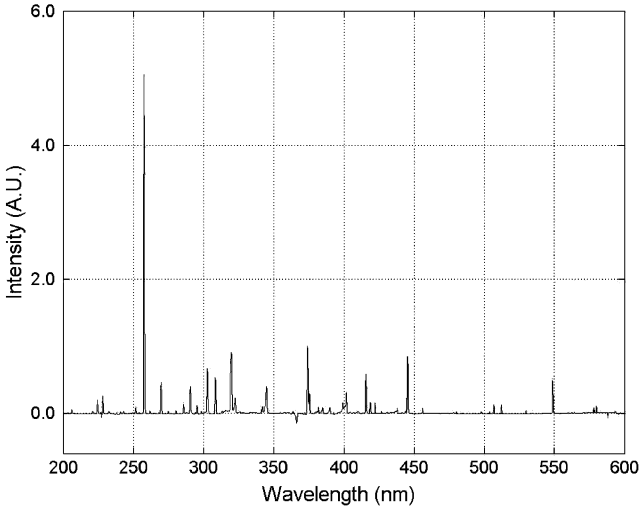

Fig. 5 Spectrum with 10.0-torr helium filling (80.0-mtorr Hg, 3.0-μs integration).

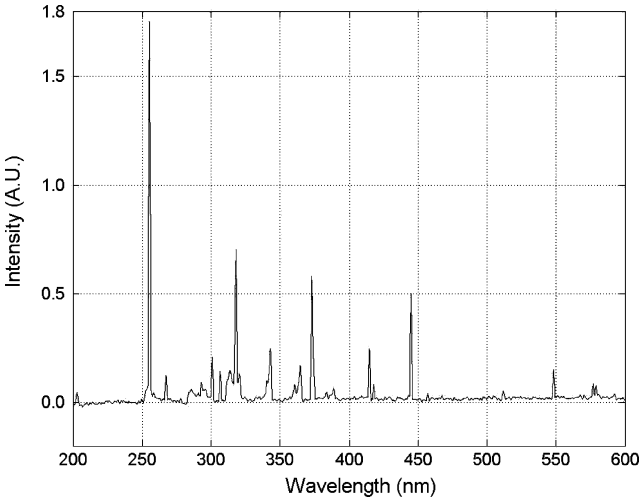

Fig. 6 Spectrum of the mercury lamp with 10.0-torr argon filling (80.0-mtorr Hg, 3.0-μs integration).

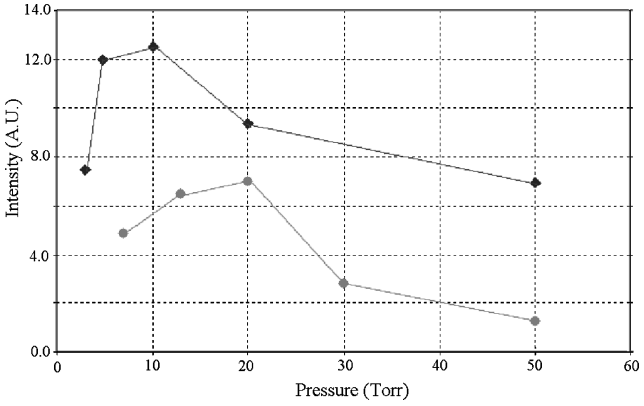

Fig. 7 Comparison of the helium filling and argon filling (80.0-mtorr Hg, 3.0-μs integration): ◆, He and ●, Ar.

A SciTech power meter was used to measure the absolute intensity of the lamp radiation. The calculation of total power was based on a linear source, 10 mm in diameter and 6.0 cm long. At a helium pressure of 10.0 torr with 80.0 mtorr of Hg pressure (with cold-tip temperature set at 80.0°C) and excitation at an 11.0-kHz pulse repetition rate with a 25.0-kV peak voltage electrical power supply, an emission intensity of 2.3 mW/cm^2 was obtained on detectors that were located a distance of 10.0 cm from the front of the 1.0-cm^2

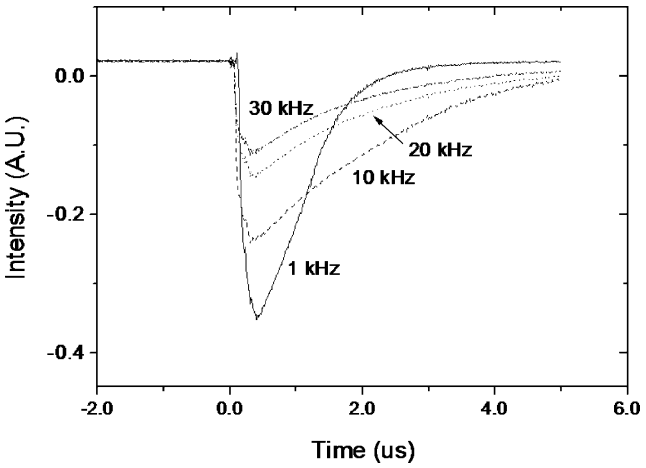

Fig. 8 Different repetition rates, 254-nm radiation (10.0-torr He, 80.0-mtorr Hg, 3.0-μs integration).

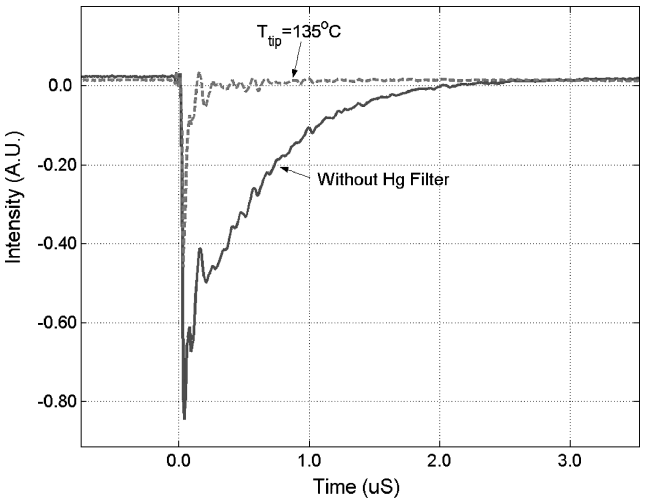

Fig. 9 Absorption by the mercury vapor filter.

optical window of the source. When the collection efficiency is included and multiplied by the total area of the lamp surface, the average total optical power of the lamp is 2.2 W. Because the repetition rate was 11.0 kHz, the energy deposition in each pulse was around 0.2 mJ. With ~10.0-μs decay time of the 254-nm line, the peak power provided by this lamp was approximately 50.0 W. To generate more power, higher-repetition-rate pulses can be applied to the discharge. This may need to be done in a pulse burst mode to avoid temperature effects.

The utility of this lamp for FRS relies on the 254-nm line remaining very narrow. For FRS to work, an optically thick mercury vapor filter must completely block the 254-nm radiation. Figure 9 shows the 254-nm line detected through a 5.0-cm-long, optically thick, mercury vapor filter. This filter consisted of an evacuated gas cell in which the mercury vapor pressure was controlled by varying the cold-tip temperature. It is apparent that the width of the 254-nm line itself is changing with time because the absorption depends on the delay time of the signal. Note from Fig. 9 that, when the tip temperature of the mercury filter was higher than 135.0°C ($P_{Hg} \sim 1.5$ torr), the unabsorbed optical signal had a decay time ~100.0 ns, which had broader linewith than the mercury vapor filter. The full absorption of the 254-nm radiation after 200.0 ns implied that the radiation was exceptionally narrow (of the order of 30.0 GHz) during this time period and that the lamp could be used for FRS measurements. Note that for commercial dc mercury lamps full absorption of the 254-nm radiation is almost impossible.

With the internal electrodes, the lifetime of the lamp was limited by the process of electrode sputtering. To overcome this problem, the lamp was redesigned to operate with external copper electrodes

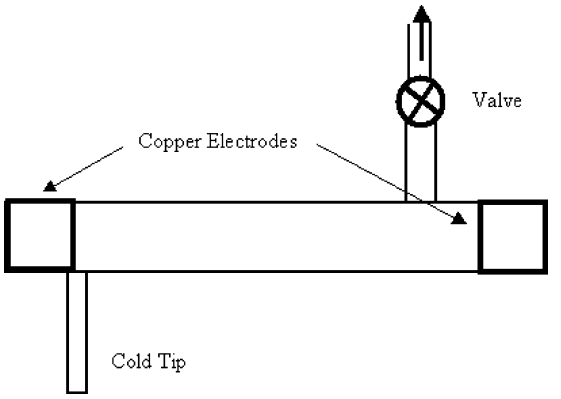

Fig. 10 Schematic of mercury vapor lamp with external electrodes.

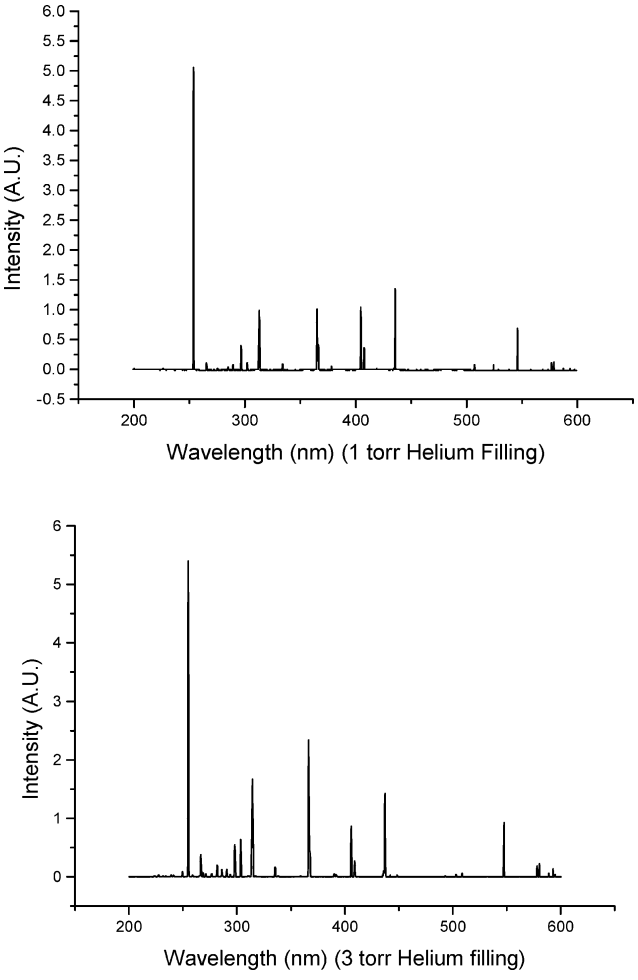

Fig. 11 Spectra at two helium pressures (80.0-mtorr Hg, 3.0-μs Integration).

(Fig. 10). Performance of this lamp was investigated at various pressures of helium and argon. Figure 11 shows the spectra for two helium pressures. Comparison of spectra for both lamps (internal and external electrodes) at 3.0-torr helium (Figs. 2 and 11) shows that the lamp with external electrodes has stronger radiation at 254 nm as compared to that with internal electrode. A more uniform and homogeneously distributed discharge was observed in case of external electrodes, whereas with internal electrodes, the discharge was mostly concentrated around the edges of the electrodes.

Figure 12 shows the pulse shapes of the 254- and 366-nm lines for various helium pressures in the external electrode lamp. It was observed that generally the decay times for lines other than 254 nm were relatively lower than those measured in the lamp with inner electrodes.

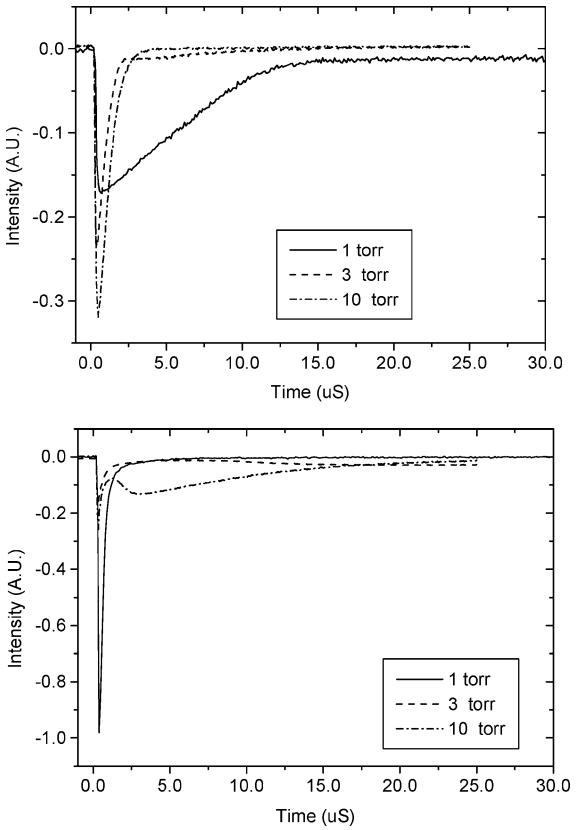

Fig. 12 Pulse shapes at 254 and 366 nm for various helium pressures.

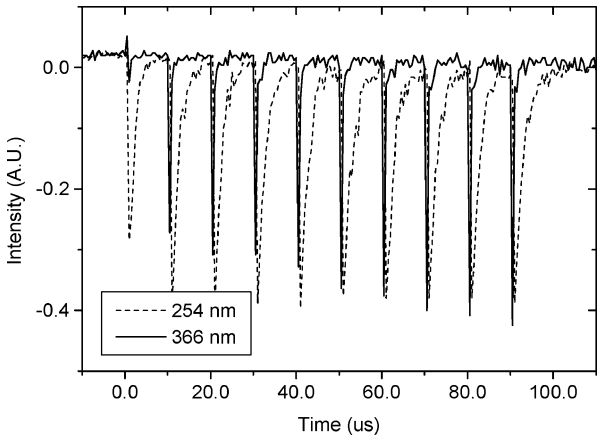

Fig. 13 Comparison of performance of pulse burst mode at 254 and 366 nm.

As mentioned earlier, the 254-nm radiation power decreases with increasing repetition rate. To increase the repetition rate without overheating, the mercury lamp was operated in the pulse burst mode, where the repetition rate of the pulse package was kept at 1.0 kHz, and 10 pulses were generated at the 100.0-kHz rate in each package. Because there were still a total of 10,000 pulses in 1 s, the heating of the lamp was similar to the uniform 10.0-kHz repetition case. Figure 13 shows the performance of the mercury lamp with external electrodes running under pulse burst mode. Although the first pulse is often weaker than other pulses, the pulse train is stable in intensity, and after the first one or two pulses, each pulse in the package is near the lamp's optimum performance.

To investigate the possible generation of 185-nm mercury line from the lamp used in the current study, some modifications were made in the data acquisition system. For the study of 185-nm radiation, a vacuum UV spectrometer photomultiplier (PMT) was employed. The SP-500 I spectrometer was modified to have the

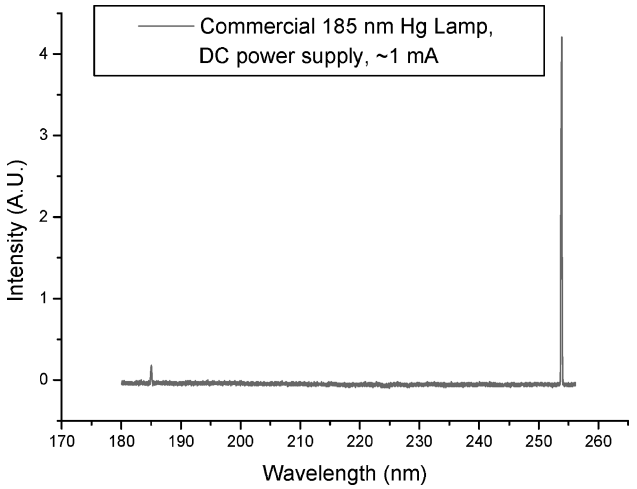

Fig. 14 Spectrum of commercial 185-nm Hg lamp with dc power supply.

capability of N_2 purging. The PMT used in the preceding experiment was replaced by another Model R7154 that has considerably higher detection efficiency below 180 nm. Both the lamp and the PMT were placed in an aluminum box that could be purged with N_2. The Hg lamp for 185-nm radiation was made from a fused silica tube, which could transmit light with wavelengths longer than 160 nm. To test the detection efficiency of the vacuum UV system, the spectrum of a commercially available 185-nm mercury lamp driven with a dc power supply was scanned. As shown in Fig. 14, the spectrum shows a 185/254-nm ratio of 1:23. From the 1:10 design ratio provided by the manufacturer, it was estimated that the detection efficiency of this system at 185 nm was roughly half of that at 254 nm. It was found that by using the pulsed power supply, the ratio of 185/254-nm radiations could be significantly increased. Figure 15 shows the comparison of 185- and 254-nm radiation at two different helium fill pressures. In both cases, the power supply was set at the 11.0-kHz repetition rate and 25.0-kV peak voltage. For 10.0-torr helium fill, with the assumption that the detection efficiency of 185 nm was one-half of that at 254 nm, the power of the lamp at 185 nm was comparable with that at 254 nm.

It was also of interest to compare the pulse shapes of the lamp at 185 and 254 nm. Figure 16 shows the pulse shapes of the lamp with a 10.0-torr helium fill. Although 185-nm radiation is also a transition to the ground state, the radiation time is much shorter. As a result, although the total power of 254 nm might be higher than 185 nm, the peak power of the 185-nm radiation is always much higher than 254-nm radiation.

IV. Applications

Because the lamp was designed to provide an ultranarrow-linewidth, UV source for high-discrimination detection, it could immediately be used as a light source in the UV region. Because the lamp radiated in all directions, it was useful to focus all of the light onto the sample under investigation. This was achieved by designing an elliptical cavity in which the sample and the lamp were located, respectively, at two foci, as shown in Fig. 17. The inner surface of the cavity was highly reflective. Because the radiation emitted by the source at one focal point must pass through the second focal point, it was anticipated that most of the radiation in the cavity would be used to illuminate the sample. The Rayleigh and Raman signals were collected from the side windows of the sample cell.

The suitability of the lamp as a UV source to perform Rayleigh and Raman measurements was tested by performing experiments with liquid and gas samples. The vibrational Raman spectrum for methanol was recorded using the experimental arrangement shown in Fig. 17.

For the methanol molecule, the O–H stretching shows very weak scattering in the Raman spectrum; only the characteristic infrared (IR) absorption could be emphasized. The CH_3 symmetric umbrella

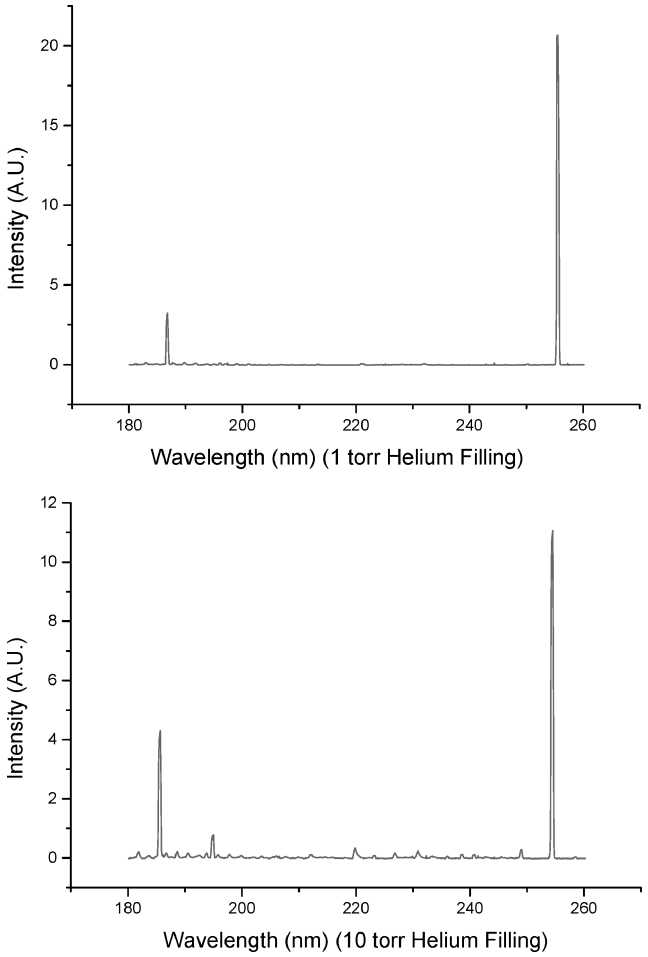

Fig. 15 Comparison of 185- and 254-nm radiation at 1.0- and 10.0-torr helium filling.

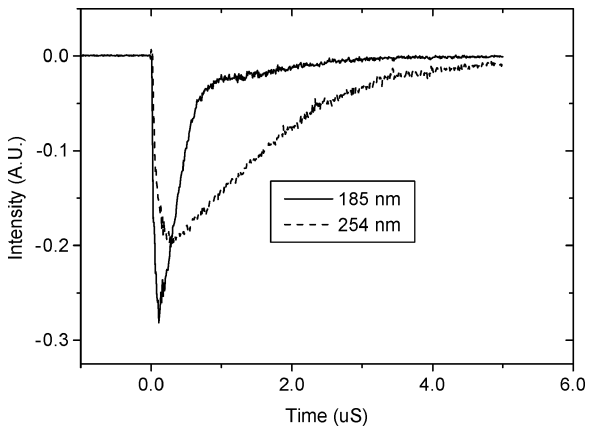

Fig. 16 Comparison of pulse shapes of 185- and 254-nm radiation (10.0-torr He, 80.0-mtorr Hg, 3.0-μs integration).

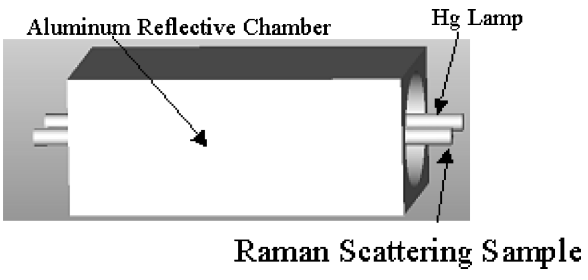

Fig. 17 Experimental setup for Raman scattering using Hg lamp.

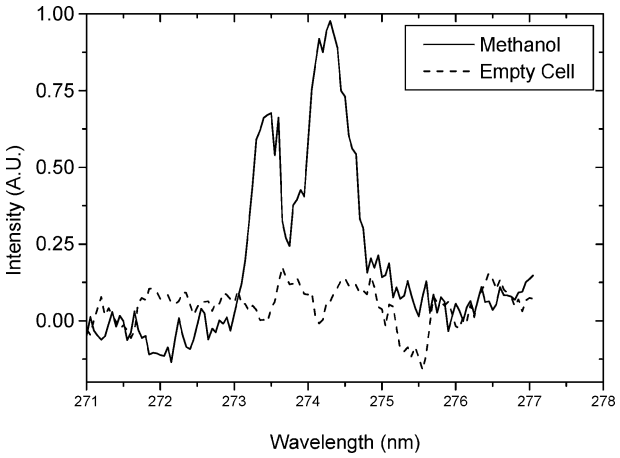

Fig. 18 Vibrational Raman scattering from methanol.

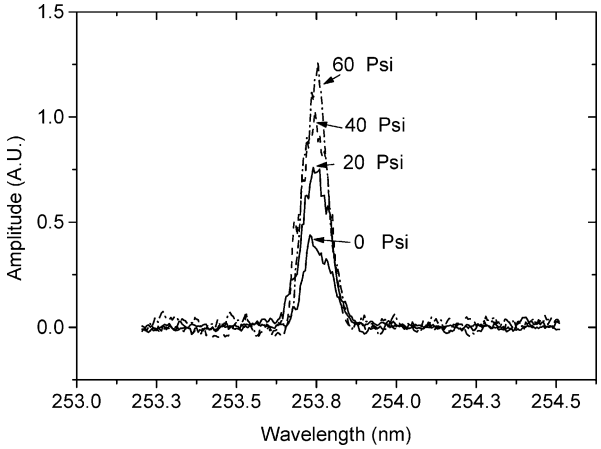

Fig. 19 FRS from CO_2 gas.

bend near 1380 cm^{-1} is medium in the IR and very weak in the Raman. The CH_3 asymmetrical and symmetrical stretchings of methanol occur near 2962 and 2872 cm^{-1}, respectively. These two lines show comparable strength in the Raman scattering and are used in this experiments. Because these vibrational Raman features appeared several nanometers away from the center frequency, there was no need to suppress the elastic scattering and the Rayleigh signal arising from the operating frequency of the lamp (254 nm). Figure 18 presents the vibrational Raman features obtained for methanol. To ensure that the lamp can be used as an alternate UV source for making Raman measurements, the vibrational Raman features observed in this study were compared and found similar to those obtained by other researchers.[17]

Measurements were also made to obtain the FRS of CO_2 gas at various pressures. Figure 19 shows the variation in the filtered Rayleigh signal as a function of the CO_2 pressure in the sample cell. The light collected from the side window of the sample cell was collimated and was passed through a Hg vapor cell before it was focused onto the spectrometer slit. Because of the resolution of the spectrometer used in these experiments, the information obtained was not used to extract any information on gas temperature. Note that the preceding experiments were conducted to demonstrate that the newly designed pulsed mercury lamp was able to provide sufficient Rayleigh and Raman signals from the gas and liquid samples used in these experiments. Future work includes the improvement in the design of the lamp to increase the peak power and the overall collection efficiency of the system.

V. Conclusions

This work presents a study of a low-pressure mercury vapor lamp, pumped by 2.0-ns, 30.0-kV voltage pulses. Preliminary results show that about 60% of the energy of the measured optical signal is at

the 254-nm line and that, after several hundred nanoseconds, the output of this lamp is virtually entirely at 254 nm. The intensity of the 254-nm emission depends on the mixture of the inert gases with the mercury. The linewidth of the 254-nm radiation, after the initial 100 ns or so, is narrow enough to be fully absorbed by an optically thick mercury vapor cell. It appears that this new kind of ultranarrow-linewidth and UV source can be used with mercury vapor filters for FRS and for other forms of high-discrimination detection. As a preliminary check, Rayleigh scattering and Raman scattering experiments have been performed with this nanosecond-pulsed mercury lamp. The performance of the lamp at 185 nm has also been studied at various conditions.

Acknowledgments

This work is supported by the Center for Molecular and Biological Imaging, which is sponsored by the State of New Jersey. We thank Michael Souza of the Princeton University Chemistry Department for the fabrication of several different kinds of Hg lamps. The efforts of Uranus Technologies, Inc., to machine the experimental hardware for this experiment are greatly appreciated.

References

[1]Forkey, J. N., Finkelstein N. D., Lempert, W. R., and Miles, R. B., "Demonstration and Characterization of Filtered Rayeigh Scattering for Planar Velocity Measurements," *AIAA Journal*, Vol. 34, No. 3, 1996, pp. 442–448.

[2]Yalin, A. P., and Miles, R. B., "Ultraviolet Filtered Rayleigh Scattering Temperature Measurements with a Mercury Filter," *Optics Letters*, 24, 590, 1999.

[3]Elliott, G. S., Boguszko, M., and Carter, C., "Filtered Rayleigh Scattering: Toward Multiple Property Measurement," AIAA Paper 2001-0301, Jan. 2001.

[4]Miles, R. B., Yalin, A., Tang, Z., Zaidi, S. H., and Forkey, J., "Flow Field Imaging Through Sharp-Edged Atomic and Molecular 'Notch' Filters," *Measurement Science and Technology*, Vol. 12, No. 4, 2001, pp. 442–451.

[5]Rothe, E. W., and Andersen, P., "Application of Tunable Excimer Lasers to Combustion Diagnostics: A Review," *Applied Optics*, Vol. 36, No. 18, 1997, pp. 3971–4033.

[6]Indralingam, R., Simeonsson, J. B., Petrucci, G. A., Smith, B. W., and Winefordner, J. D., "Raman-Spectrometry with Metal Vapor Filters," *Analytical Chemistry*, Vol. 64, No. 8, 1992, pp. 964–967.

[7]Nohe, A., Lermann, G., Schwoerer, H., Kiefer, W., Sawatzki, J., and Surawicz, G., "High Resolution Low Wavenumber Fourier Transform Raman Spectroscopy with a Rubidium Vapor Filter and a Ti:Sapphire Laser," *Journal of Molecular Spectroscopy*, Vol. 65, 1997, pp. 410, 411.

[8]Tang, Z., "Infra-Red Rubidium Atomic Resonant Filters for Low Wavenumber Scattering," Ph.D. Dissertation, Dept. of Mechanical and Aerospace Engineering, Princeton Univ., Princeton, NJ, June 2001.

[9]Finkelstein, N. D., Lempert, W. R., and Miles, R. B., "Rotational Raman Scattering Measurements with a Single Mode Laser Source and Narrow Passband Filter," *Optics Letters*, Vol. 22, No. 8, 1997, p. 537.

[10]Catalog of VCCD512, High Speed Scientific Grade Camera, Sarnoff Corporation, 2003.

[11]Waymouth, J. F., *Electric Discharge Lamps*, MIT Press, Cambridge, MA, 1971, pp. 11–46.

[12]Milenin, V. M., and Timofeev, N. A., "Electron Relaxation to a Maxwellian Energy Distribution in the Positive Column of a Low-Pressure Mercury Discharge," *Soviet Physics—Technical Physics [Zhurnal Tekhnicheskoi Fiziki]*, Vol. 23, No. 9, 1978, pp. 1048–1051.

[13]Milenin, V. M., and Timofeev, N. A., "On the Possibility of Enhancing the Luminous Efficacy of Low-Pressure Discharge Sources," *Svetotekhnika*, Vol. 4, April 1981, pp. 6–8.

[14]Milenin, V. M., Panasyuk, G. Y., and Timofeev, N. A., "Physical Properties of the Plasma of Low-Current Steady-State and Periodic-Pulse Discharges in Mixtures of a Metal Vapor and an Inert Gas," *Soviet Journal of Plasma Physics*, Vol. 12, No. 4, 1986, pp. 258–261.

[15]Vasilyak, L. M., Krasnochub, A. V., Kuz'menko, M. E., and Kostyuchenko, S. V., "Excitation of the 6(3)P(1) Atomic Level of Mercury by Pumping a Mixture of Mercury Vapor and Argon with a Pulse-Periodic Nanosecond Discharge," *Technical Physical Letters*, Vol. 24, No. 3, 1998, p. 205.

[16]Massey, G. A., and Lemon, C. J., "Feasibility of Measuring Temperature and Density-Fluctuations in Air Using Laser-Induced O-2 Fluorescence," *IEEE Journal of Quantum Electronics*, Vol. QE-20, No. 5, 1984, pp. 454–457.

[17]McClain, B. L., Clark, S. M., Gabriel, R. L., and Ben-Amotz, D., "Educational Applications of IR and Raman Spectroscopy: A Comparison of Experiment and Theory," *Journal of Chemical Education*, Vol. 77, No. 5, 2000, p. 654.

J. Trolinger
Guest Editor